Heat Flow and Thermal Source of the Xi'an Depression, Weihe Basin, Central China

Wei Xu[1]*, Xiaoyin Tang[2]*, Luyao Cheng[1], Ying Dong[3], Yuping Zhang[4], Tingting Ke[1], Ruyang Yu[5] and Yi Li[6]

[1]Institute of Global Environmental Change, Xi'an Jiaotong University, Xi'an, China, [2]Institute of Geomechanics, Chinese Academy of Geological Sciences, Beijing, China, [3]Xi'an Center of China Geological Survey, Xi'an, China, [4]Key Laboratory of Coal Resources Exploration and Comprehensive Utilization, Ministry of Land and Resources, Xi'an, China, [5]School of Earth Resources, China University of Geosciences, Wuhan, China, [6]Sichuan Institute of Geological Engineering Investigation Group Co. Ltd., Chengdu, China

The Xi'an Depression of the Weihe Basin, located in the transition zone where the North China, Qinling and Yangtze plates collide with each other, is an important area of geothermal energy utilization in China. Studies of heat flow and thermal sources are of great significance to the exploration and development of geothermal resources in this area. In this paper, six temperature logs boreholes, and 14 thermal conductivity samples have been used to study the geothermal gradient and terrestrial heat flow in the area. The results show that the geothermal gradients of Xi'an Depression range from 20.8 C/km to 49.1 C/km, with an average of 31.7 ± 5.0 C/km. The calculated heat flow is 59.4–88.6 mW/m^2, and the average value is 71.0 ± 6.3 mW/m^2, which indicates a high thermal background in the area. The high anomalous zones are near the Lintong-Chang'an Fault zone in the southeast, the Weihe Fault in the north, and the Fenghe Fault in the central Xi'an Depression. These deep and large faults not only control the formation of the Xi'an Depression but also provide an important channel for the circulation of groundwater and affect the characteristics of the shallow geothermal distribution. The temperature of the Moho in the Xi'an Depression ranges from 600 to 700°C, and the thermal lithosphere thickness is about 90–100 km. The characteristics of lithospheric thermal structure in Xi'an Depression indicate that the higher thermal background in the study area is related to lithospheric extension and thinning and asthenosphere thermal material upwelling.

Keywords: geothermal gradient, heat flow, thermal sources, xi'an depression, weihe basin

INTRODUCTION

Terrestrial heat flow is the basis for the study of the regional thermal background (Jiang et al., 2019; Wang et al., 2020; Xu et al., 2021), geothermal resource evaluation (Ciriaco et al., 2020), and tectono-thermal evolution (Qiu et al., 2014; Zuo et al., 2020; Chang et al., 2021; Jiang et al., 2021).

The Weihe Basin is situated between the southwestern margin of the North China Plate and the Qinling Orogenic Belt (**Figure 1**). It is a half-graben rift basin controlled by its southern and northern bounding faults and filled with 7,000 m Cenozoic sediments (Rao et al., 2014). The Weihe Basin has a great geothermal resource exploration potential. The history of geothermal development and utilization in this area can be traced back to Huaqin Hot Springs in the Tang Dynasty (Stober and Bucher, 2013). Based on the results of geology, tectonics, geophysics, and geochemistry, etc.,
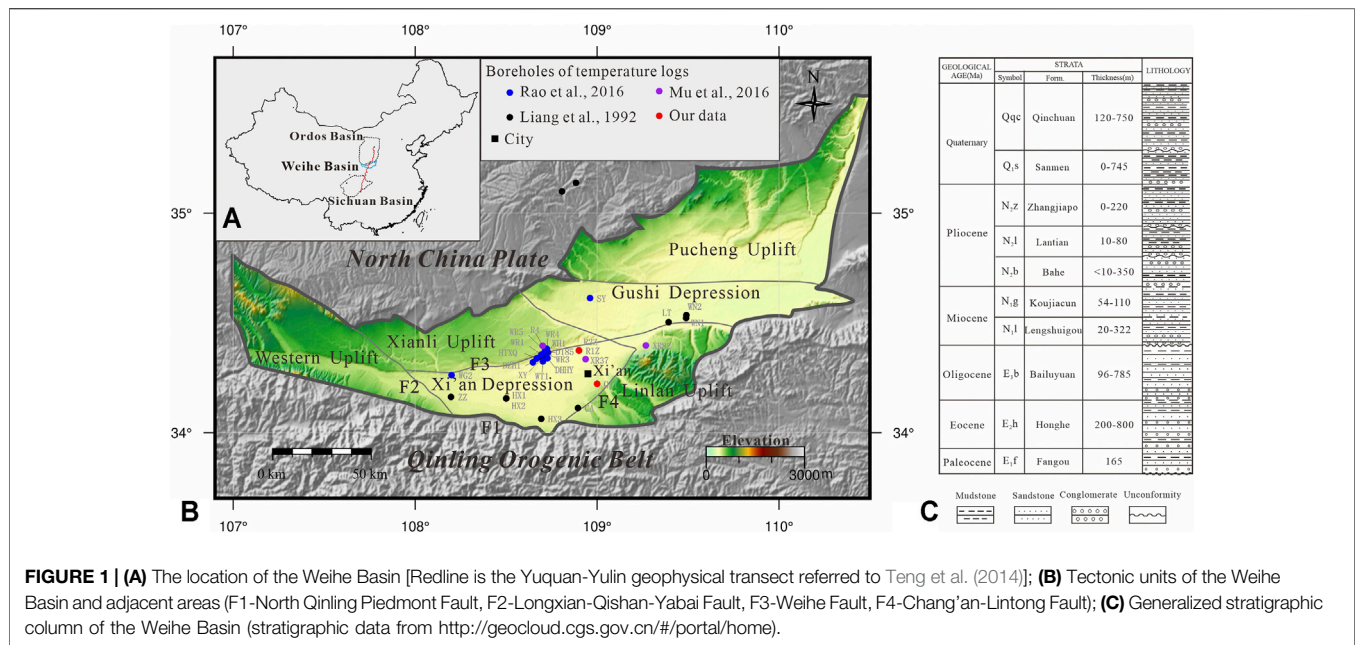
FIGURE 1 | (A) The location of the Weihe Basin [Redline is the Yuquan-Yulin geophysical transect referred to Teng et al. (2014)]; **(B)** Tectonic units of the Weihe Basin and adjacent areas (F1-North Qinling Piedmont Fault, F2-Longxian-Qishan-Yabai Fault, F3-Weihe Fault, F4-Chang'an-Lintong Fault); **(C)** Generalized stratigraphic column of the Weihe Basin (stratigraphic data from http://geocloud.cgs.gov.cn/#/portal/home).

previous studies have been conducted on the characteristics of the geothermal field (Rao et al., 2016; Ren et al., 2020), the characteristics of underground hot water (Qin et al., 2005a; Ma et al., 2008b) the evaluation of geothermal resources (Mu et al., 2016; Zhang et al., 2020), and the characteristics of the thermal structure of the lithosphere in the Weihe Basin (Rao et al., 2016; Liang et al., 1992).

The Xi'an Depression is a secondary tectonic unit of the Weihe Basin. It is the main area for the exploration and utilization of geothermal resources. However, most of the temperature log boreholes are concentrated in Xianyang City. The accurate determination of the geothermal field and the further study of controlling factors in the Xi'an Depression (such as fault structures and groundwater circulation systems) are restricted. In addition, the Xi'an Depression developed many deep faults, but different researchers have disputes over whether these deep faults control thermal anomalies (Rao et al., 2016; Deng et al., 2017). Therefore, the thermal background and the mechanism of thermal anomalies in the Xi'an Depression still need to be strengthened.

In this paper, we used temperature logs data from six boreholes and 14 thermal conductivity data and studied the geothermal gradient and heat flow of the Xi'an Depression combined with data collected from the previous studies (Liang et al., 1992; Rao et al., 2016). Then, the relationship between heat flow and faults and groundwater circulation is studied, and the mechanism of regional thermal background is discussed. The research is of great significance for understanding the distribution characteristics of geothermal resources and thermal sources in the Xi'an Depression.

GEOLOGICAL SETTING

The Xi'an Depression is the main tectonic unit of the Weihe Basin, located in the central and southern parts of the basin

(**Figure 1A**). The west is bounded by the Longxian-Qishan-Yabai Fault and adjacent to the Western Uplift; the north is separated by the Weihe Fault and adjacent to the Xianli Uplift; the east is bounded by the Chang'an-Lintong Fault and adjacent to the Linlan Uplift; the south is adjacent to the Qinling Orogenetic Belt separated by the North Qinling Piedmont Fault.

The basement of the Xi'an Depression mostly consists of Proterozoic metamorphic rocks (Wang H et al., 2010). The Paleogene includes the Honghe Formation (E_2h), the Bailuyuan Formation (E_3b); the Neogene includes the Lengshuigou Formation (N_1l), the Koujiacun Formation (N_1k), the Bahe Formation (N_2b), the Lantian Formation (N_2l), the Zhangjiapo Formation (N_2z) and the Quaternary strata. These sedimentary units consisted of an alternation of sandstone and mudstone layers (**Figure 1B**) (Liu and Xue, 2004).

The Xi'an Depression is located at the intersection of China's east-west tectonic divisions and north-south tectonic divisions. It is a complex transition zone where the Qinling Orogenetic Belt, the North China Block, and the Yangtze Block collide with each other. Before the Early Cretaceous, the Xi'an Depression belonged to the southern margin of the Ordos paleo-continent and was dominated by subsidence and sedimentation. It experienced three tectonic evolutionary stages during the Late Ordovician to Early Cretaceous, including the Caledonian, the Hercynian, and the Late Indo-East Yanshanian tectonic activities (Zhao and Liu, 1990; Yang, 2002). In the Caledonian, tectonic compression occurred in the study area, resulting in the overall uplift and denudation. In the Hercynian, the study area was further compressed, and uplift occurred in the south and depression occurred in the north. During the Late Indo-East Yanshanian, the Weihe Basin was uplifted widely, and the deformation of the northern margin of the Weihe Basin was strengthened, and the compressive deformation zone was extended northward. Since the early cretaceous, the formation of the northern margin of the

TABLE 1 | Thermal conductivity for the rocks from the Xi'an Depression.

Well no	Depth (m)	Lithology	Thermal conductivity (W/(mK))		References
			measured	corrected	
XS1	113.60	Sandstone	1.92	2.17	Our data
XS2	160.60	Sandstone	1.88	2.13	
XG1	117.00	Clay	1.94	2.19	
XG2	100.00	Clay	1.67	1.92	
XG3	47.00	Clay	1.61	1.86	
XG4	67.00	Clay	1.63	1.88	
XS3	101.60	Clay	1.89	2.14	
XS4	79.40	Clay	1.84	2.09	
XS5	140.70	Clay	1.68	1.93	
XU1		Mudstone	2.11	2.32	Luo, (2015)
XU2		Mudstone	1.68	1.89	
XU3		Sandstone	2.41	2.62	
XU4		Sandstone	3.24	3.45	
XU5		Sandstone	3.03	3.25	

Qinling Orogenetic Belt caused by the northward overthrust under the control of the north-south compressive stress has become an important tectono-thermal event (Liu et al., 2006). Since the Cenozoic, the Xi'an Depression has turned into an extension environment. It can be divided into four stages: rifting stage in the Eocene-Oligocene, uplifting stage in the late Oligocene-early Miocene, subsidence stage in the middle Miocene-Pliocene and the same for the Quaternary (Han et al., 2002; Liu et al., 2006; Liu et al., 2010; Wang J et al., 2010).

METHODS AND DATA

Thermal Conductivity

Thermal conductivity is an important parameter for studying heat flow, lithospheric thermal structure, and temperature distribution inside the Earth (Wang, 2016). In this paper, a total of nine core samples from the Quaternary strata in the Xi'an Depression were sampled for thermal conductivity testing. The samples were measured using the TCS (Thermal Conductivity Scanning) technique by LGM-Lippmann Company (Popov et al., 2016). It has a measurement range of 0.2–25.0 W/(mK) with a measurement resolution of 0.001 W/(mK). The accuracy is ±3% on individual samples. These samples were measured at room temperature conditions, and each sample was tested three times to take the average value.

Combined with the collected data (Luo, 2015), a total of 14 rock thermal conductivity data were obtained (**Table 1**). The results show that the thermal conductivity of Xi'an Depression range from 1.61 W/(mK) to 3.24 W/(mK), with an average value of 2.04 ± 0.49 W/(mK).

The factors affecting the thermal conductivity of rocks mainly include water saturation, porosity, and mineral composition (Brigaud et al., 1990; Pribnow et al., 1996; Jougnot and Revil, 2010). Since the testing data are derived from dry rock samples, it is necessary to consider the water saturation calibration. In this study, the thermal conductivity data are corrected by using the water saturation method (Yu et al., 2020).

TABLE 2 | Thermal conductivity of the sedimentary strata in the Xi'an Depression.

Formation	Lithology	n	Thermal conductivity [W/(m·K)]		
			Range	Harmonic mean	Mixing value
Q	Clay	7	1.86–2.19	1.99 ± 0.12	2.03 ± 0.10
	Sandstone	2	2.13–2.17	2.15 ± 0.02	
N	Mudstone	2	1.89–2.32	2.08 ± 0.22	2.29 ± 0.25
	Sandstone	3	2.62–3.45	3.07 ± 0.35	

The mixing value is the thermal conductivity calculated from different lithology and the thickness of the lithology in the stratum.

According to the geological data of the Xi'an Depression, the average porosity of the formations of N_2l-N_2b, N_1l-N_1g, E_3b is 22.2, 20.3, and 16.5%, respectively (Huang et al., 2021). According to the trend of porosity distribution with depth, we assume that the porosity of Quaternary is about 25.0%. Then, the results of the dry rock samples measured at the laboratory are corrected (**Table 1**). The corrected thermal conductivity ranges from 1.86 W/(mK) to 3.45 W/(mK), the average value is 2.28 ± 0.48 W/(mK). The corrected value is about 12% higher than the measured value.

Combined with the lithological thickness ratios (Huang et al., 2021) and weighted harmonic mean thermal conductivity of each lithology, the thermal conductivity of different formations can be calculated. We established a thermal conductivity column for sedimentary strata in the Xi'an Depression (**Table 2**). The mean bulk thermal conductivity of the Neogene is 2.29 ± 0.25 W/(mK), and the Quaternary is 2.03 ± 0.10 W/(mK).

Temperature Logs

The temperature of the sedimentary basin is mainly based on the temperature measurement data from the drilling boreholes, which can reflect the true condition of the geothermal field in the basin. In this study, high-quality precision temperature logs of three boreholes in the Xi'an Depression were measured (**Figure 1**). These boreholes have been stopped production for

FIGURE 2 | Temperature logs of the boreholes in the Xi'an Depression [R4, HS, LS refers from Mu et al. (2016)]
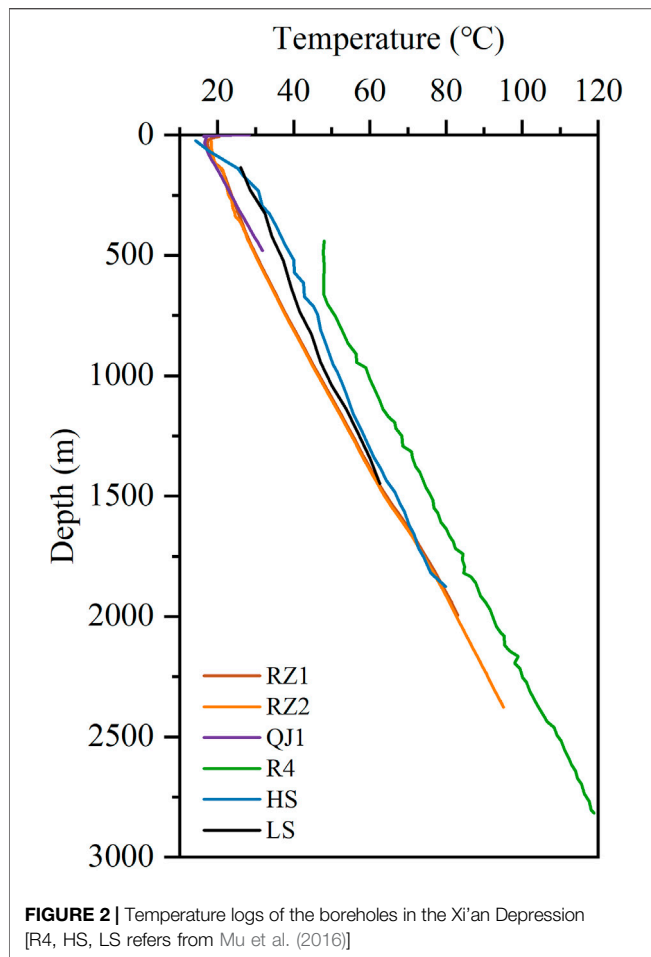
more than 1 year, and the temperature has reached thermal equilibrium.

The equipment for the borehole temperature logging operation of R1Z and R2Z is made by Spartek Systems, Canada. It has a measurement sensitivity of 0.001°C, a depth interval of temperature recording of 10 cm, and a temperature measurement range from 0 to 150°C. The equipment used in QJ1 is the DEFI Series made by the JFE Advantech Co., Ltd, Japan, with a measurement resolution of 0.001°C, a temperature measurement interval of 0.15 cm, and a temperature measurement range of −3–45 °C.

Figure 2 shows the systematical temperature logging curves (temperature-depth profile) of the three boreholes. The depth section of R1Z ranges from 6 to 1996 m, corresponding to a temperature range of 20–83°C; The R2Z is measured from 25 to 2,377 m with a temperature range of 18.4–95.1°C (Zhang et al., 2019). The depth of QJ1 is 0–480 m with a temperature range of 16.3–31.8°C. The study also collected temperature logs data from three boreholes (Mu et al., 2016), with a maximum depth of 2,830 m and a maximum temperature of 119.0°C. Except that the shallow temperature is affected by climate or convection of groundwater, the temperature curve generally increases linearly with depth, indicating that the heat transfer method is

conductive type, which can be used to characterize the present thermal field characteristics of the Xi'an Depression.

RESULTS

Geothermal Gradient

Geothermal gradient is the rate of temperature change with depth and is the crucial parameter for calculating the heat flow value. To obtain an accurate geothermal gradient, we have considered many factors, such as climate change, the convection of groundwater, and the effect of stratigraphic stratification. This paper selected relatively stable temperature intervals and used the least-square regression method to calculate the geothermal gradients for different layers, and the correlation coefficients are all above 99% (**Table 3**). The results show that the geothermal gradient ranges from 27.5 to 37.6 C/km, with an average value of 32.7 ± 7.0 C/km. It is lower than that of Songliao Basin in northeast China (37.0 C/km) (Wu and Xie, 1985), and consistent with that of Bohai Bay Basin in east China 32.8 C/km (Hu et al., 2001; Gong, 2003; Qiu et al., 2009), and higher than the stable basins in central and western China, Sichuan Basin 22.7 C/km (Xu et al., 2011), Tarim Basin 22.6 C/km (Feng et al., 2009), Junggar Basin 21.3 C/km (Rao et al., 2013) and Qaidam Basin 28.6 C/km (Li et al., 2015).

The spatial pattern of geothermal gradient was analyzed by considering the above data and data from previous studies (**Figure 3**; **Table 3**) (Liang et al., 1992; Rao et al., 2016). The geothermal gradient of the Xi'an Depression is about 20.8–49.1 C/km, with an average of 31.7 ± 5.0 C/km. **Figure 3** shows that most regions of the Xi'an Depression have geothermal gradients greater than 30 C/km, and the southwest and eastern parts are lower than 30 C/km. High anomalous zones occur in the northern and central-southern parts of the area with geothermal gradients of about 35–50 C/km.

Heat Flow

Terrestrial heat flow is equal to the product of the thermal conductivity and the vertical geothermal gradient. The geothermal gradient can be calculated by systematical steady-state temperature data, which are measured in the drilled borehole. The thermal conductivity of rock samples in the corresponding depth intervals can be tested in the laboratory. With these two parameters, we can obtain heat flow values. Its mathematical expression is:

$$q = K \frac{dT}{dZ} \qquad (1)$$

where q is the heat flow (mW/m^2); K is the rock thermal conductivity [W/(mK)]; dT/dZ is the geothermal gradient (°C/km).

The standard deviation of heat flow depends on standard deviations of the rock thermal conductivity and geothermal gradient. The heat flow uncertainty is calculated as:

$$\sigma_q = \sqrt{G^2 \sigma_K^2 + K \sigma_G^2} \qquad (2)$$

TABLE 3 | Geothermal gradients and heat flow data of the Weihe Basin.

Well no	Longitude	Latitude	Form	Depth (m)	Gradient (°C/km)	K [W/(m·K)]	Heat flow (mW/m²)		References
							section	average	
R1Z	108.90043	34.37635	Q	329–1,016	32.2 ± 0.1	2.03 ± 0.10	65.4 ± 3.2	75.7 ± 6.3	Our data
			N	1,016–1979	37.6 ± 0.1	2.29 ± 0.25	86.1 ± 9.4		
R2Z	108.90028	34.37670	Q	312–1,014	32.2 ± 0.1	2.03 ± 0.10	65.4 ± 3.2	74.0 ± 6.1	
			N	1,014–2,377	36.1 ± 0.1	2.29 ± 0.25	82.7 ± 9.0		
QJ1	108.99980	34.22450		99–480	34.8 ± 0.1	2.03 ± 0.10	70.6 ± 3.5	70.6 ± 3.5	
R4	108.70089	34.39828		703–2,816	33.0 ± 0.1	2.16 ± 0.19	71.3 ± 6.3	71.3 ± 6.3	
HS	108.93662	34.33698		335–1816	28.0 ± 0.3	2.16 ± 0.19	60.5 ± 5.3	60.5 ± 5.3	
LS	109.26804	34.39929		147–1,455	27.5 ± 0.5	2.16 ± 0.19	59.4 ± 5.3	59.4 ± 5.3	
YX1	108.80722	35.09806			20.8	3.19 ± 0.23		66.4 ± 0.5	Liang et al. (1992)
YX2	108.88417	35.13722		1,330–2089	23.4 ± 0.3	2.84 ± 0.37		66.3 ± 8.6	
ZZ	108.19667	34.16444			28.4 ± 0.5	2.43 ± 0.25		69.0 ± 7.3	
HX2	108.50028	34.15750		500–2,650	29.5 ± 0.2	2.43 ± 0.25		71.6 ± 7.5	
HX3	108.69306	34.06389		475–900	31.9 ± 0.5	2.43 ± 0.25		77.5 ± 8.2	
XY	108.69889	34.34222			49.1 ± 0.7	1.45 ± 0.20		71.2 ± 9.9	
CA	108.89472	34.11361			31.1 ± 0.7	2.43 ± 0.25		75.6 ± 8.1	
LT	109.39333	34.50583			31.0 ± 0.2	2.08 ± 0.31		64.6 ± 9.5	
WN1	109.48917	34.52472			32.0 ± 0.2	2.08 ± 0.30		66.4 ± 9.7	
WN2	109.49056	34.53778			28.5 ± 0.1	2.19 ± 0.32		62.5 ± 9.1	
WH1	108.72583	34.36972		360–1,150	34.8	2.11		73.4	Rao et al. (2016)
WR1	108.69278	34.35750		450–2,720	33.4	2.40		80.2	
WR3	108.71889	34.36500		520–2,710	29.6	2.43		71.9	
WR4	108.72361	34.38417		480–2,820	31.5	2.43		76.5	
WR5	108.71278	34.37333		530–1,600	32.6	2.21		72.0	
D185	108.73032	34.36708		510–1,390	29.4	2.18		64.1	
SY	108.96139	34.61528		180–1,140	32.3	2.08		67.2	
WT1	108.70222	34.32722		380–1740	40.1	2.21		88.6	
DHHY	108.72694	34.34167		360–1938	30.6	2.24		68.5	
HTXQ	108.66778	34.34028		520–2,700	30.4	2.43		73.9	
WG2	108.20028	34.26389		480–1,250	35.8	2.15		77.0	
DZH1	108.64722	34.32278		320–1,010	34.3	2.10		72.0	
					31.7 ± 5.0			71.0 ± 6.3	

K: Thermal conductivity.

where G is geothermal gradient; σ_K and σ_G are standard deviations of the rock thermal conductivity geothermal gradient.

In this study, based on the above temperature logs data and measured thermal conductivity data, the heat flow values of the six boreholes were calculated (**Table 3**). The results show that the maximum heat flow of the six boreholes is 75.7 ± 6.3 mW/m², the minimum is 59.4 ± 5.3 mW/m², and the average heat flow is 68.6 ± 3.6 mW/m². It is close to that of Songliao Basin in northeast China 70.9 mW/m² (Jiang et al., 2019), and slightly higher than that of Bohai Bay Basin 64.3 ± 14.7 mW/m² (Gong et al., 2011; Jiang et al., 2019), much higher than Tarim Basin in western China 43.0 mW/m² (Feng et al., 2009), Sichuan Basin 53.2 mW/m² (Xu et al., 2011), Junggar Basin 42.5 mW/m² (Rao et al., 2013) and Qaidam Basin 55.1 mW/m² (Li et al., 2015).

Combined with heat flow data from previous studies (**Table 3**) (Liang et al., 1992; Rao et al., 2016), the spatial pattern of heat flow was analyzed (**Figure 3**). The heat flow values in Xi'an Depression range from 59.4 to 88.6 mW/m², and the average heat flow is 71.0 ± 6.3 mW/m², which is significantly higher than the average continental heat flow of 60.4 ± 12.3 mW/m² in China (Jiang et al., 2016). **Figure 3** shows that the northern and central south parts are the high anomalous zones with high heat flow of

70–90 mW/m², and the southwest and eastern parts are low heat flow areas of 60–70 mW/m².

DISCUSSION

Factors Influencing the Distribution of Thermal Anomalies

Faults are the main factors affecting the distribution of geothermal anomalies in the Xi'an Depression. Many fault structures are developed in the Xi'an Depression. The fault structures can be divided into four groups according to their distribution directions, EW direction, NE direction, NW direction, and NNE direction (**Figure 4**) (Li et al., 1994; Mu et al., 2016). Among them, the faults of EW, NE, and NW trending are the most developed and constitute the basic structural framework of the study area. The southern part of the Xi'an Depression is the EW-trending North Qinling Piedmont Fault (F1) and Yuxia-Tieluzi Fault (F2), the NE-trending Weihe Fault (F3) in the north, the NW-trending Yabai Fault (F6) in the west, the NNW-trending Fenghe Fault (F7) in the central part, the NW-trending Jinghe Fault (F11) in
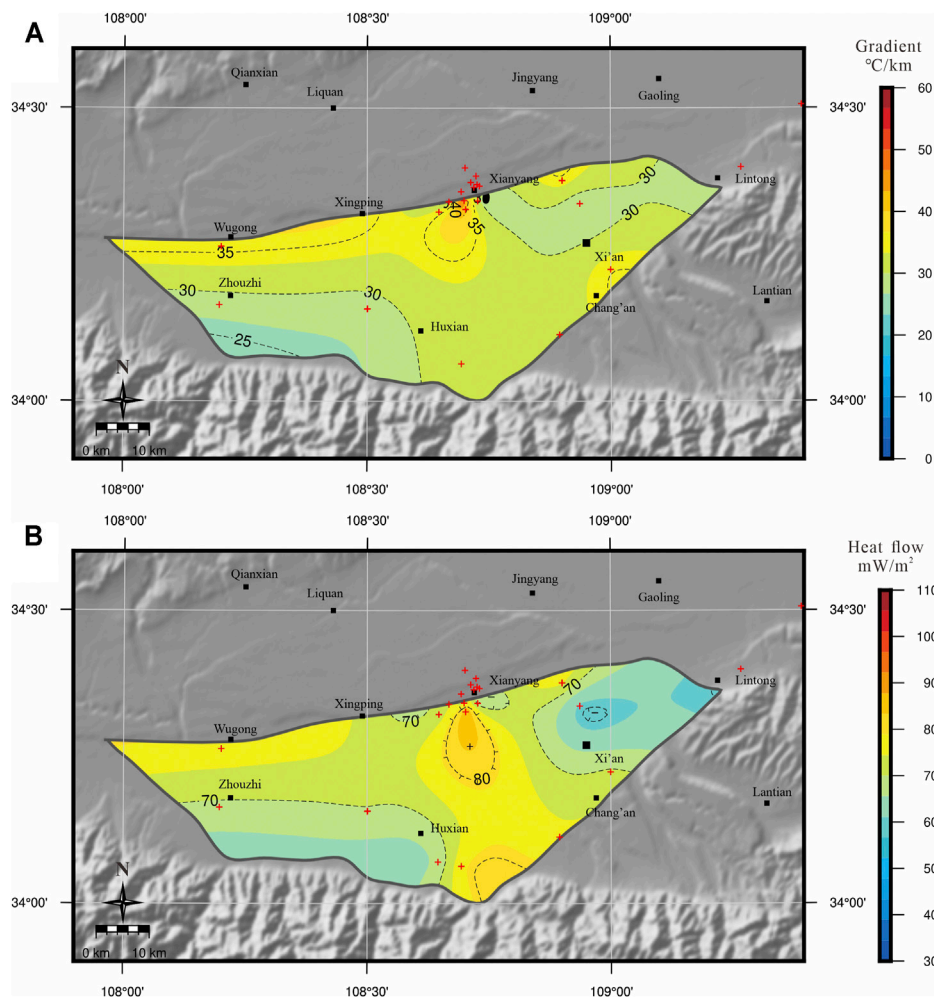
FIGURE 3 | Contour maps of the geothermal gradient **(A)** and heat flow **(B)** of the Xi'an Depression and adjacent areas. Red crosses show the locations of the geothermal measurements.

the northeast, and the NNE-trending Lintong-Changan Fault (F12) in the southeast. These deep faults not only control the formation of the Xi'an Depression but also provide an important channel for the circulation of groundwater and affect the characteristics of the geothermal distribution. **Figure 4** shows the relationship between heat flow distribution and faults. In the southern part of the Xi'an Depression, the high heat flow zone corresponds to the NNE-trending Lintong-Chang'an fault zone (F12); in the northern part, the high heat flow zone corresponds to the NE-trending Weihe fault (F3); the central high-heat flow zone corresponds to the NNW-trending Fenghe fault (F7).

Groundwater circulation is important to the distribution of geothermal anomalies in the Xi'an Depression. The geothermal reservoirs of the Weihe Basin are recharged by rain that falls on the northern slope of the Qinling Mountains, North Mountains, and the pediment surface water (Qin et al., 2005b; Ma et al., 2008b; Luo, 2015). The low heat flow of the eastern area of the depression may relate to the mix of water from the Qinling Mountains, water from Weibei, local surface water, and ground

cold water (Li and Li, 2010). Two geothermal water reservoirs may be distinguished in the Weihe Basin; they are circulating (current) geothermal reservoirs and isolated (fossil) geothermal reservoirs (Ma et al., 2008a; Ma et al., 2008b). The host environments of the geothermal water of Xianyang and Xi'an are belonging to an isolated geothermal reservoir at a depth deeper than 1,500 m. Groundwater circulation depth is an important parameter in the research of the geothermal field. It is estimated that the circulation depth of geothermal water in the Xianyang geothermal system can reach 4,900 m based on the temperature of the geothermal reservoir and geothermal gradient (Luo, 2015). Hydrogen and oxygen isotope evidence show that the geothermal water in Xianyang is supplied by atmospheric precipitation in the Qinling mountains, and the noble gas isotope $^3He/^4He$—$^4He/^{20}Ne$ indicate that the fluid circulation occurs only in the crust depth and is not supplemented by mantle-derived materials (Luo et al., 2019). Therefore, we believe that the geothermal water in Xi'an Depression mainly receives the atmospheric precipitation of the Qinling Mountains, forming
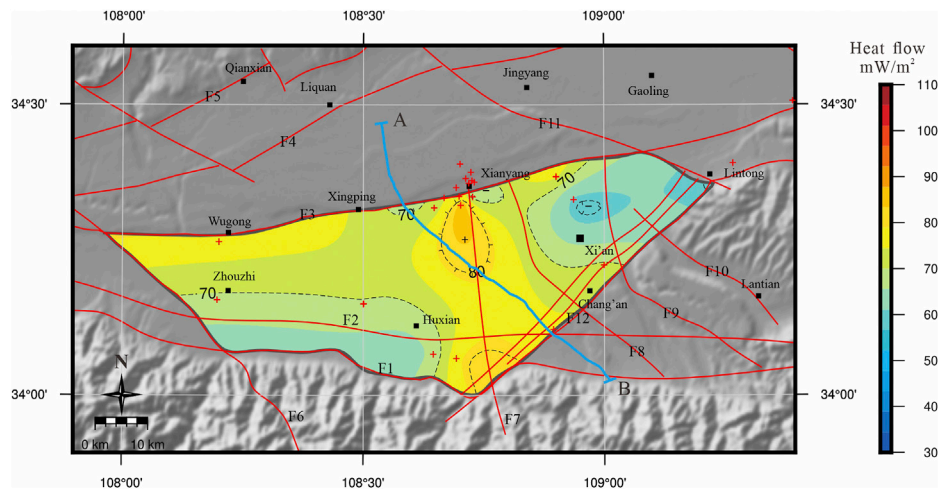
FIGURE 4 | The relationship between heat flow distribution and faults in Xi'an Depression [(A,B): deep seismic reflection survey profile (Ren et al., 2013); F1-North Qinling Piedmont Fault, F2-Yuxia-Tieluzi Fault, F3-Weihe Fault, F4-Liquan-Shuangquan fault, F5-Qianxian-Fuping Fault, F6-Yabai Fault, F7-Fenghe Fault, F8-Zaohe Fault, F9-Chanhe Fault, F10-Bahe fault, F11-Jinghe Fault, F12-Lintong-Changan Fault].
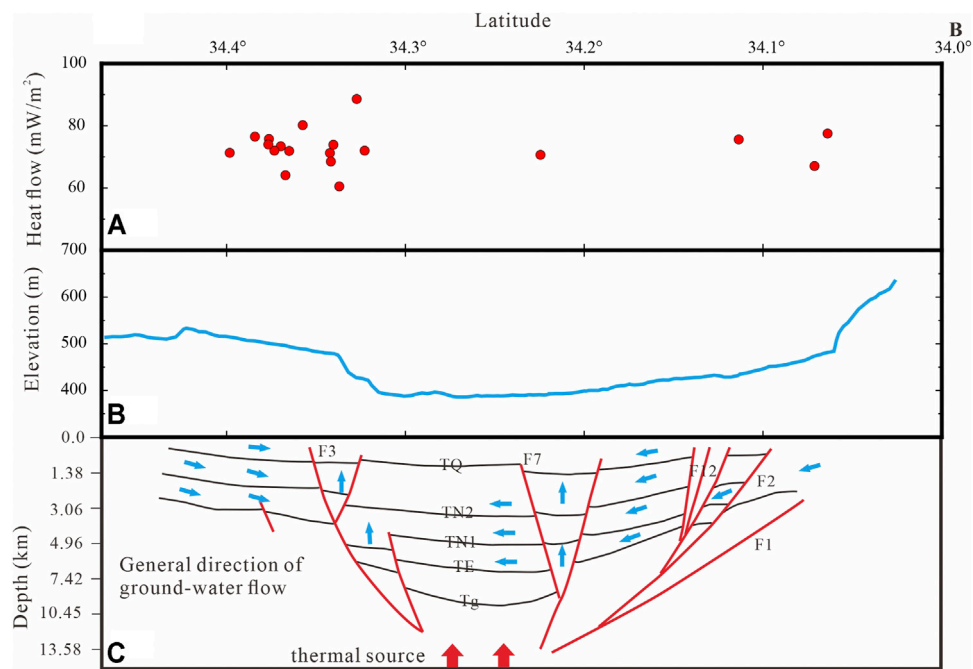
FIGURE 5 | Heat flow **(A)**, elevation **(B)** and Schematic diagram of deep structure and water flow direction **(C)** (Ma et al., 2008b; Ren, 2012; Ren et al., 2013) observed and calculated response along the geophysical transect [**(A,B)** transect can be seen in **Figure 4**] (TQ is the bottom boundary of the Quaternary Formation, TN1 and TN2 are the reflected waves of the new Tertiary Formations, TE is the bottom boundary of the old Tertiary Formation, and the reflected wave Tg may be the top boundary of the crystalline basement).

circulating geothermal reservoirs in the deep part of the Weihe fault and the Lintong-Chang'an fault zone, and forming isolated geothermal reservoir in the central part of the Xi'an Depression (**Figure 5**). The shallow area is still dominated by heat conduction. Circulating geothermal reservoirs are controlled

by open fractures, the geothermal water mixes with atmospheric precipitation moving downwards during the process of moving upward along the open fractures. Isolated geothermal reservoirs are mainly characterized by high temperature and high pressure and are distributed deep in the
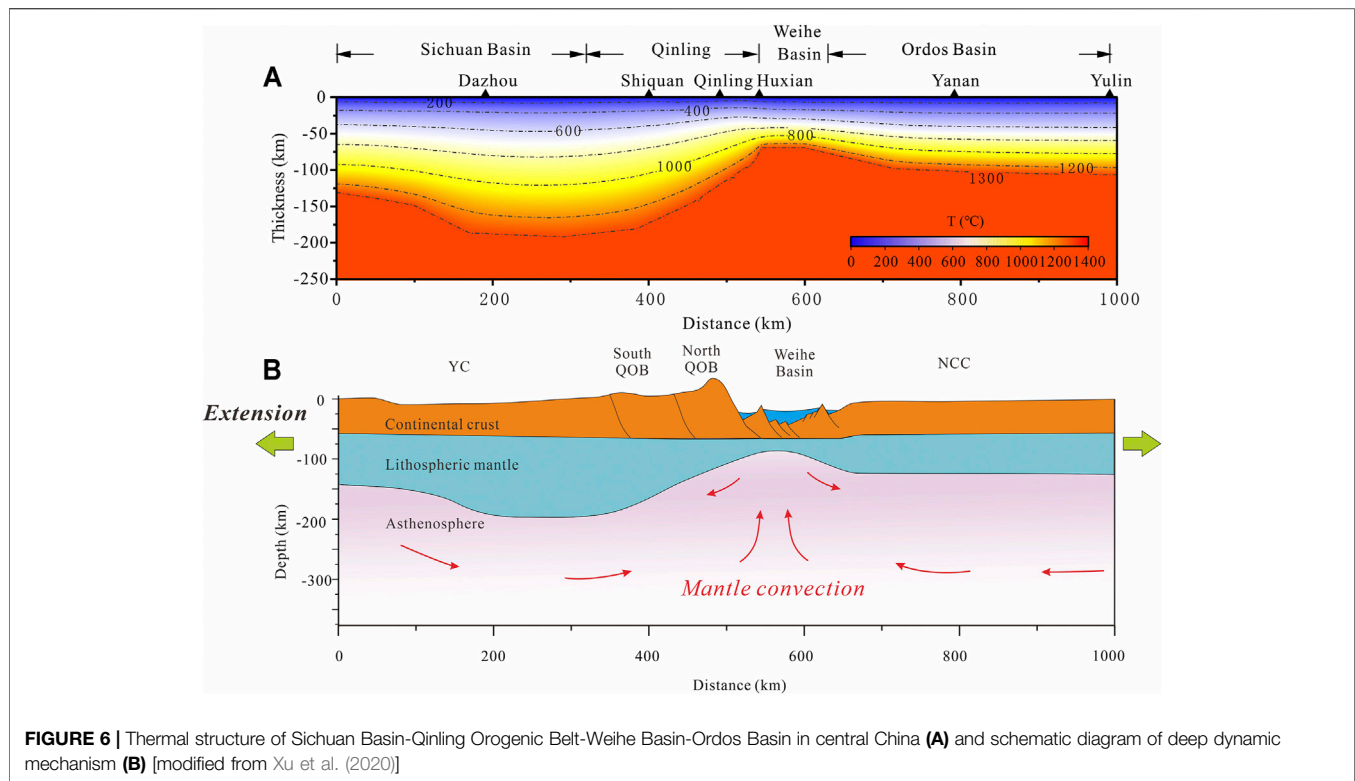
FIGURE 6 | Thermal structure of Sichuan Basin-Qinling Orogenic Belt-Weihe Basin-Ordos Basin in central China **(A)** and schematic diagram of deep dynamic mechanism **(B)** [modified from Xu et al. (2020)]

middle of the basin. The upward migration of deep geothermal water not only affects the geothermal field near the fault zone, but may also affect the formations on both sides of the fault, causing the temperature higher than normal, and forming a high heat flow anomalous zone near the deep fault.

The thickness of the sedimentary layer is also a factor affecting the geothermal anomalies. The sediment source areas of Xi'an Depression are from the Qinling and Weibei uplifts. The topographic features of this depression show an increasing trend on the whole from north to south, and the sediment filling gradually thickens to the north (**Figure 5**). According to the analysis of thermal reservoir, the thicker the reservoir rock bodies is, the more favorable it is to store hot water. Therefore, the thermal anomalies in the north are more significant than those in the south.

Thermal Source of the Xi'an Depression

Tectonic activity can change the thermal state of the crustal or lithosphere. The range and magnitude of the thermal state of the crustal or lithosphere changed by tectonic activity are mainly controlled by the combined effects of thermal relaxation, changes in the lithospheric heat generation rate, and tectonic processes (Furlong and Chapman, 2013). As the lithospheric thinning and crustal extension, affected by the equilibrium effect, the deep thermal matter rises, which increases the surface heat flow. The higher heat flow in the Weihe Basin belongs to the thermal effect of the crustal extension and thinning event (Xu et al., 2020). Based on the 2-D profile of the Yuquan-Yulin seismic reflection transect,

we used the finite element method (Litmod-2D) (Afonso et al., 2008) to measure the elevation, Bouguer gravity, geoid height, heat flow, mantle composition, crustal and lithospheric structure as constraints to simulate the thermal structure of the continental lithosphere in the Sichuan Basin-Qinling Orogenic Belt-Ordos Basin (Xu et al., 2020). According to the distribution characteristics of the temperature field in the deep part of the profile, the temperature of the Moho in the Xi'an Depression ranges from 600 to 700°C, and the thermal lithosphere thickness is about 90–100 km (**Figure 6**). The results show that the Weihe Basin has a thin lithosphere and is affected by the thermal upwelling of the asthenosphere, resulting in a high thermal background in the study area.

Since the Cenozoic, the Xi'an Depression has turned into an extensional environment, beginning the development period of extensional fault basin, and it is still in the extensional stage at present (Han et al., 2002; Liu et al., 2006;Liu et al., 2010; Wang H et al., 2010). Therefore, the Xi'an Depression is in a state where the lithosphere and crust are stretched and thinned, resulting in a higher heat flow. Its deep geodynamic mechanism may be influenced by intracontinental deformation of the Yangtze and North China Plates in the Late Mesozoic, the far-field effect of the collision between the Indian Plate and the Eurasian Plate, and the eastward extrusion of the Qinghai-Tibetan Plateau (**Figure 6**). Based on the strong intracontinental deformation of the Yangtze and North China Plates in the Late Mesozoic, combined with the far-field effect of the collision between the Indian Plate and the Eurasian Plate and the eastward extrusion of Qinghai-Tibetan

Plateau, the deep part of the Qinling orogenic belt is still squeezed from north to south, and accompanying the uplift of the Qinling Mountains and the subsidence of the Weihe Basin in the north (Zhang et al., 1996; Zhang et al., 1997; Wang et al., 2003; Meng et al., 2005; Meng, 2017). As a result, the Xi'an Depression is in a continuous tensile stress field, the depression continues to subsidence, the lithosphere is thinned, and the upwelling of asthenosphere thermal materials further deepens the lithosphere thinning and leading to high heat flow.

CONCLUSION

1) The geothermal gradient of the Xi'an Depression in the Weihe Basin is 20.8–49.1 °C/km, with an average value of 31.7 ± 5.0 °C/km. The heat flow ranges from 59.4 to 88.6 mW/m^2, and the average heat flow is 71.0 ± 6.3 mW/m^2, which is significantly higher than the average continental heat flow of 60.4 ± 12.3 mW/m^2 in China.
2) The results of heat flow indicate that the Xi'an Depression belongs to a high thermal background area. The high heat flow zones are related to faults and groundwater circulation. The geothermal anomalous areas are near the Lintong-Chang'an fault zone in the south, the Weihe fault in the north, and the Fenghe fault in the central part of the depression.
3) The high thermal background in this area is related to the influence of the strong intracontinental deformation of the Yangtze and North China Plates in the Late Mesozoic, the far-field effect of the collision between the Indian Plate and the Eurasian Plate, and the eastward extrusion of Qinghai-Tibetan Plateau. The Xi'an Depression is in a continuous tensile stress field, the lithosphere is thinned, and the upwelling of thermal materials further deepens the lithosphere thinning, leading to high heat flow.

REFERENCES

Afonso, J. C., Fernàndez, M., Ranalli, G., Griffin, W. L., and Connolly, J. A. D. (2008). Integrated Geophysical-Petrological Modeling of the Lithosphere and Sublithospheric Upper Mantle: Methodology and Applications. *Geochem. Geophys. Geosyst.* 9, a–n. doi:10.1029/2007GC001834

Brigaud, F., Chapman, D. S., and Le Douaran, S. (1990). Estimating thermal Conductivity in Sedimentary Basins Using Lithologic Data and Geophysical Well Logs (1). *AAPG Bull.* 74 (9), 1459–1477. doi:10.1306/0c9b2501-1710-11d7-8645000102c1865d

Chang, J., Glorie, S., Qiu, N., Min, K., Xiao, Y., and Xu, W. (2021). Late Miocene (10.0~6.0 Ma) Rapid Exhumation of the Chinese South Tianshan: Implications for the Timing of Aridification in the Tarim Basin. *Geophys. Res. Lett.* 48 (3), e2020G–e90623G. doi:10.1029/2020GL090623

Ciriaco, A. E., Zarrouk, S. J., and Zakeri, G. (2020). Geothermal Resource and reserve Assessment Methodology: Overview, Analysis and Future Directions. *Renew. Sust. Energ. Rev.* 119, 109515. doi:10.1016/j.rser.2019.109515

Deng, Y., Ren, Z., and Ren, W. (2017). Geothermal Distribution Control Factors and Geothermal prospect in Guanzhong Region. *Land Dev. Eng. Res.* 2 (11), 19–27.

Feng, C.-G., Liu, S.-W., Wang, L.-S., and Li, C. (2009). Present-Day Geothermal Regime in Tarim Basin, Northwest China. *Chin. J. Geophys.* 52, 1237–1250. doi:10.1002/cjg2.1450

Furlong, K. P., and Chapman, D. S. (2013). Heat Flow, Heat Generation, and the thermal State of the Lithosphere. *Annu. Rev. Earth Planet. Sci.* 41, 385–410. doi:10.1146/annurev.earth.031208.100051

Gong, Y.-l., Zhang, H., and Ye, T.-f. (2011). Heat Flow Density in Bohai bay basin: Data Set Compilation and Interpretation. *Proced. Earth Planet. Sci.* 2, 212–216. doi:10.1016/j.proeps.2011.09.034

Gong, Y. L. (2003). *The thermal Structure and thermal Evolution of Bohai Bay Basin Eastern China.*

Han, H., Zhang, Y., and Yuan, Z. (2002). The Evolution of Weihe Down-Faulted basin and the Movement of the Fault Blocks. *J. Seismological Res.* 4 (25), 362–368.

Hu, S., O'Sullivan, P. B., Raza, A., and Kohn, B. P. (2001). Thermal History and Tectonic Subsidence of the Bohai Basin, Northern China: A Cenozoic Rifted and Local Pull-Apart basin. *Phys. Earth Planet. Interiors* 126, 221–235. doi:10.1016/S0031-9201(01)00257-6

Huang, J., Zhou, Y., Teng, H., Liang, X., Gao, J., Cao, X., et al. (2021). On the Occurrence Characteristics and the Estimation of Geothermal Water in Xi'an Sag,guanzhong basin. *Northwest. Geology.* 54 (1), 196–203.

Jiang, G., Gao, P., Rao, S., Zhang, L., Tang, X., Huang, F., et al. (2016). Compilation of Heat Flow Data in the china continental Area (4rd Edition). *Chin. J. Geophys.* 44, 2892–2910.

Jiang, G., Hu, S., Shi, Y., Zhang, C., Wang, Z., and Hu, D. (2019). Terrestrial Heat Flow of continental China: Updated Dataset and Tectonic Implications. *Tectonophysics* 753, 36–48. doi:10.1016/j.tecto.2019.01.006

DATA AVAILABILITY STATEMENT

The original contributions presented in the study are included in the article/supplementary material, further inquiries can be directed to the corresponding authors.

AUTHOR CONTRIBUTIONS

WX: Conceptualization, Investigation, Methodology, Software, Writing—Original Draft, Writing—Review and Editing, Formal analysis, Visualization XT: Conceptualization, Writing—Review and Editing, Supervision LC: Investigation, Methodology, Software, Data Curation YD: Investigation, Resources YZ: Investigation, Resources TK: Investigation, Writing—Reviewing RY: Investigation, Methodology, Data Curation YL: Investigation, Data Curation.

FUNDING

ACKNOWLEDGMENTS

Jiang, S., Zuo, Y., Yang, M., and Feng, R. (2021). Reconstruction of the Cenozoic Tectono-thermal History of the Dongpu Depression, Bohai bay basin, china: Constraints from Apatite Fission Track and Vitrinite Reflectance Data. *J. Pet. Sci. Eng.* 205, 108809. doi:10.1016/j.petrol.2021.108809

Jougnot, D., and Revil, A. (2010). Thermal Conductivity of Unsaturated clay-rocks. *Hydrol. Earth Syst. Sci.* 14 (1), 91–98. doi:10.5194/hess-14-91-2010

Li, G., and Li, F. (2010). *The Circulation Law and Sustainable Utilization of Ground Hot Water in Guanzhong basin*. Beijing: China Science Publishing & Media LTD.

Li, T., Xu, J., and Ren, G. (1994). Study on Geomechanical Modelling of the Fault Activites in Xi'an Area. *J. Eng. Geology.* 2 (3), 34–42.

Li, Z., Gao, J., Zheng, C., Liu, C., Ma, Y., et al. (2015). Present-day Heat Flow and Tectonic-thermal Evolution since the Late Paleozoic Time of the Qaidam basin. *Chin. J. Geophys.* 58, 3687–3705.

Liang, S., Sun, T., Han, Y., and Shi, S. (1992). Terrestrial Heat Flow in the 4th Geoscience Transection of china. *Sci. Bull.* 37 (2), 143–146.

Liu, C., Zhao, H., Gui, X., Yue, L., Zhao, J., and Wang, J. (2006). Space-time Coordinate of the Evolution and Reformation and Mineralization Response in Ordos basin. *Acta Geologica Sinica* 80 (5), 637–646.

Liu, H., and Xue, X. (2004). Discussion on the Cenozoic and its Chronology in the Weihe River basin. *J. Earth Sci. Enivronmental* 26 (4), 1–5.

Liu, J. H., Zhang, P. Z., Zheng, D. W., Wan, J. L., and Wang, W. T. (2010). The Cooling History of Cenozoic Exhumation and Uplift of the Taibai Mountain, Qinling, china: Evidence from the Apatite Fission Track(aft) Analysis. *Chin. J. Geophys.* 53 (10), 2405–2414. doi:10.1007/s11430-010-0016-0

Luo, L. (2015). *Genesis and Reservoir Modification Analysis of Xianyang Geothermal System, Guanzhong basin*. [dissertation]. [Beijing]: University of Chinese Academy of Sciences.

Luo, L., Zhu, X., He, C., Mao, X., Xu, Z., Wang, X., et al. (2019). Study on the Genesis of Geothermal Fluid in Xianyang Geothermal Field. *Geol. Rev.* 65 (6), 1422–1430.

Ma, Z., Wang, X., Su, Y., and Yu, J. (2008b). Oxygen and Hydrogen Isotope Exchange and its Controlling Factors in Subsurface Geothermal Water S in the central Guanzhong basin, Shaanxi, china. *Geol. Bull. China* 27 (6), 888–894.

Ma, Z., Yu, J., Li, Q., Wang, X., Li, F., Mu, G., et al. (2008a). Environmental Isotope Distribution and Hydrologic Geologic Sense of Guanzhong basin Geothermal Water. *J. Earth Sci. Environ.* 30 (4), 396–401.

Meng, Q.-R., Wang, E., and Hu, J.-M. (2005). Mesozoic Sedimentary Evolution of the Northwest Sichuan basin: Implication for Continued Clockwise Rotation of the south china Block. *Geol. Soc. America Bull.* 117 (3-4), 396. doi:10.1130/B25407.1

Meng, Q. (2017). Origin of the Qinling Mountains. *Scientia Sinica Terrae* 47 (4), 412–420.

Mu, G., Li, F., Yan, W., and Li, C. (2016). *Occurrence Rules and Key Technologies of Exploitation and Utilization of Geothermal Resources in Guanzhong basin*. Beijing: Geological Publishing House.

Popov, Y., Beardsmore, G., Clauser, C., and Roy, S. (2016). Isrm Suggested Methods for Determining thermal Properties of Rocks from Laboratory Tests at Atmospheric Pressure. *Rock Mech. Rock Eng.* 49 (10), 4179–4207. doi:10.1007/s00603-016-1070-5

Pribnow, D., Williams, C. F., Sass, J. H., and Keating, R. (1996). Thermal Conductivity of Water-Saturated Rocks from the KTB Pilot Hole at Temperatures of 25 to 300°C. *Geophys. Res. Lett.* 23 (4), 391–394. doi:10.1029/95gl00253

Qin, D., Turner, J. V., and Pang, Z. (2005a). Hydrogeochemistry and Groundwater Circulation in the Xi'an Geothermal Field, China. *Geothermics* 34 (4), 471–494. doi:10.1016/j.geothermics.2005.06.004

Qin, D., Turner, J. V., and Pang, Z. (2005b). Hydrogeochemistry and Groundwater Circulation in the Xi'an Geothermal Field, china. *Geothermics* 34 (4), 471–494. doi:10.1016/j.geothermics.2005.06.004

Qiu, N., Wei, G., Li, C., Zhang, Y., and Guo, Y. (2009). Distribution Features of Current Geothermal Field in the Bohai Sea Waters. *Oil Gas Geology.* 30, 412–420.

Qiu, N., Zuo, Y., Chang, J., and Li, W. (2014). Geothermal Evidence of Meso-Cenozoic Lithosphere Thinning in the Jiyang sub-basin, Bohai bay basin, Eastern north china Craton. *Gondwana Res.* 26 (3-4), 1079–1092. doi:10.1016/j.gr.2013.08.011

Rao, G., Lin, A., Yan, B., Jia, D., and Wu, X. (2014). Tectonic Activity and Structural Features of Active Intracontinental normal Faults in the Weihe Graben, central china. *Tectonophysics* 636, 270–285. doi:10.1016/j.tecto.2014.08.019

Rao, S., Hu, S., Zhu, C., Tang, X., Li, W., et al. (2013). The Characteristics of Heat Flow and Lithospheric thermal Structure in Junggar Basin, Northwest China. *Chin. J. Geophys.* 56, 2760–2770.

Rao, S., Jiang, G. Z., Gao, Y. J., Hu, S. B., and Wang, J. Y. (2016). The thermal Structure of the Lithosphere and Heat Source Mechanism of Geothermal Field in Weihe basin. *Chin. J. Geophys.-Ch.* 59 (6), 2176–2190.

Ren, J., Feng, X., Wang, F., Peng, J., Liu, C., Dai, W., et al. (2013). Fine Crust Structures of Xi'an Sag in the Weihe basin Revealed by a Deep Seismic Reflection Profile. *Chin. J. Geophys.* 56 (2), 513–521.

Ren, J. (2012). *Probe on the Deep Crustal Structure in Weihe basin and Tectonics Research of basin*. [dissertation]. [Xi'an]. Chang'an University.

Ren, Z., Liu, R., Ren, W., Qi, K., Yang, G., Cui, J. et al. (2020). Distribution of Geothermal Field and its Controlling Factors in the Weihe basin. *Acta Geologica Sinica* 94 (7), 1938–1949. doi:10.1111/1755-6724.14458

Stober, I., and Bucher, K. (2013). History of Geothermal Energy Use from Theoretical Models to Exploration and Development. *Springer Berlin Heidelberg*, 15–24. Berlin, Heidelberg. doi:10.1007/978-3-642-13352-7_2

Teng, J. W., Li, S. L., Zhang, Y. Q., Wang, F. Y., Pi, J. L., et al. (2014). Fine Velocity Structures and Deep Processes in Crust and Mantle of the Qinling Orogenic Belt and the Adjacent North China Craton and Yangtze Craton. *Chin. J. Geophys.* 57, 3154–3175.

Wang, E., Meng, Q., Clark Burchfiel, B., and Zhang, G. (2003). Mesozoic Large-Scale Lateral Extrusion, Rotation, and Uplift of the Tongbai-Dabie Shan belt in east China. *Geol* 31 (4), 307. doi:10.1130/0091-7613(2003)031<0307:mlsler>2.0.co;2

Wang, H., Liu, B., Ma, Z., Li, Y., and Jin, W. (2010). Analysis of Distribution of Geophysical Characteristics and Reservoir-Forming Conditions in the Pre-cenozoic Strata in the Weihe basin. *Prog. Geophys.* 25 (4), 1280–1287.

Wang, J. (2016). *Geothermics and its Applications*. Beijing: Science Press.

Wang, J., Liu, C., Yan, J., Zhao, H., Gao, F., and Liu, C. (2010). Development Time and Evolution Characteristics of Weibei Uplift in the South of Ordos basin. *J. Lanzhou Univ. (Natural Sciences)* 46 (4), 22–29.

Wang, Y., Wang, L., Hu, D., Guan, J., Bai, Y., Wang, Z., et al. (2020). The Present-Day Geothermal Regime of the north Jiangsu basin, east china. *Geothermics* 88, 101829. doi:10.1016/j.geothermics.2020.101829

Wu, Q., and Xie, Y. (1985). Geothermal Heat Flow in the Songhuajiang-Liaoning Basin. *Seismology Geology.* 7, 59–64.

Xu, M., Zhu, C.-Q., Tian, Y.-T., Rao, S., and Hu, S.-B. (2011). Borehole Temperature Logging and Characteristics of Subsurface Temperature in the Sichuan Basin. *Chin. J. Geophys.* 54, 224–233. doi:10.1002/cjg2.1604

Xu, W., Huang, S., Zhang, J., Zuo, Y., Zhou, Y., Ke, T., et al. (2021). Geothermal Gradient and Heat Flow of the Erlian basin and Adjacent Areas, Northern china: Geodynamic Implication. *Geothermics* 92, 102049. doi:10.1016/j.geothermics.2021.102049

Xu, W., Li, Y., Zhou, L., Ke, T., and Cheng, L. (2020). Lithospheric thermal Regime under the Qinling Orogenic belt and the Weihe basin: a Transect across the Yangtze and the north china Cratons in central china. *Tectonophysics* 789, 228514. doi:10.1016/j.tecto.2020.228514

Yang, J. (2002). *Ordos basin Tectonic Evolution and Hydrocarbon Distribution Rule*. Beijing: Petroleum Industry Press.

Yu, R., Huang, S., Zhang, J., Xu, W., Ke, T., Zuo, Y., et al. (2020). Measurement and Analysis of the thermal Conductivities of Rocks Samples from the Baiyinchagan Sag and Uliastai Sag, Erlian basin, Northern china. *Acta Petrol. Sin.* 36 (2), 621–636.

Zhang, G., Meng, Q., Liu, S., and Yao, A. (1997). Huge Intracontinental Subduction Zone at South Margin of north china Block and Present 3-d Lithospheric Framework of the Qinling Orogenic belt. *Geol. J. Univ.* 3 (2), 129–143.

Zhang, G. W., Meng, Q. G., Yu, Z. P., Sun, Y., Zhou, D. W., and Guo, A. L. (1996). Orogenesis and Dynamics of the Qinling Orogen. *Sci. China Ser. D-Earth Sci.* 39 (3), 225–234. doi:10.1360/yd1996-39-3-225

Zhang, J., Dong, M., Wang, B., Ai, Y., and Fang, G. (2020). Geophysical analysis of geothermal resources and temperature structure of crust and upper mantle beneath guanzhong basin of shaanxi,china. *Journal Earch Sci. Environ.* 43 (1), 150–163.

Zhang, Y., Huang, S., Yang, F., Wang, X., Yu, R., Li, Y., et al. (2019). Geothermal Features of Two Deep U-Shape Downhole Heat Exchangers in the Xi'an Depression,guanzhong basin. *Coal Geology. China* 31 (6), 54–61.

Zhao, Z., and Liu, C. (1990). The Formation and Evolution of the Sedimentary Basins and Their Hydrocarbon Occurrence in the north china Craton. *Xi'an: Northwest. Univ. Press* 53 (5), 2–5. (in Chinese).

Zuo, Y., Jiang, S., Wu, S., Xu, W., Zhang, J., Feng, R., et al. (2020). Terrestrial Heat Flow and Lithospheric thermal Structure in the Chagan Depression of the Yingen-Ejinaqi Basin, north central China. *Basin Res.* 32 (6), 1328–1346. doi:10.1111/bre.12430